phosphate dehydrogenase (GAPDH) was quantitatively measured in all samples as the internal control. The GAPDH primer and probe sequences were as follows: forward primer, CCATCACTGCCACTCAGAAGAC; reverse primer, TCATACTTGGCAGGTTTCTCCA; and probe, CGTGTTCCTACCCCCAATGTATCCGT.

All TaqMan RT-PCR data was captured with Sequence Detector Software (SDS version 1.7; PE Applied Biosystems, Weiterstadt, Germany). The mRNA/GAPDH value for each sample was calculated, followed by calculation of the induction value for comparison with the normal rat mRNA/GAPDH level.

Statistical Analysis

Data are expressed as mean ± standard deviation (SD). The Mann-Whitney *U* test was performed using Stat View (Version 4, SAS Institute, Cary, NC) for comparisons of the control and PP1 groups. The *p*-values of <0.05 were considered significant.

RESULTS

Extent of Contusional Lesions

After recovery from anesthesia, all animals were paraplegic. HE-stained sections demonstrated that on day 1 the location of the contusional lesions coincided with the location of the compression. On days 3 and 7, inflammatory cells had infiltrated the area of the contusion and its immediate surround. The areas of the contusional lesions of the control group measured 5.56 ± 1.29 mm^2 ($n = 14$) and of the PP1 group 5.50 ± 1.19 mm^2 ($n = 12$) on day 1. Because there was no significant difference, it was assumed that the severity of the primary damage was essentially the same in both groups. On day 3, however, the injured areas of the control group and the PP1 group were 7.79 ± 3.32 mm^2 ($n = 16$) and 5.06 ± 1.19 mm^2 ($n = 16$), respectively, showing a significant reduction (approximately 35%) in the PP1 group compared to the control group ($p < 0.01$). Although the areas of the contusional lesions of both groups were reduced on day 7 as compared to day 3, they showed the same pattern as that reported on day 3 (data not shown).

VEGF Expression

On days 3 and 7 after compression, marked VEGF protein expression was detected in the neurons and glial cells surrounding the contusional lesion in both the control and PP1 groups. This expression was most intense on day 3. There was no significant difference between the two groups in terms of VEGF expression (Fig. 1).

Extent of Edema

The extent of edema was investigated first with the aid of the anti-IgG antibody. The area of edema of the PP1 group on day 1 after compression was considerably reduced compared with that of the control group (Fig. 2). The water content of the spinal cord on days 1, 3, and 7 is shown in Figure 3. The water content was 66.86 ± 1.78% in nonoperated normal animals ($n = 6$). Spinal cord compression increased the water content to 71.81 ± 1.31% on day 1 after compression (control group, $n = 6$) whereas those rats administered PP1 had a water content of 70.06 ± 0.45% (PP1 group, $n = 6$). On day 3, the water content in the control group was 74.66 ± 1.54% ($n = 4$) and 72.23 ± 0.60% ($n = 4$) in the PP1 group, indicating that, compared with day 1, edema was aggravated in both groups. On day 7, however, the corresponding values were 70.73 ± 0.32% ($n = 5$) and 69.75 ± 0.50% ($n = 4$), showing that in both groups edema was reduced compared with day 3 values. On days 1, 3, and 7, the *p*-values were 0.0163, 0.0202, and 0.0127, respectively, indicating a statistically significant difference between the two groups.

Macrophage Infiltration

Macrophages infiltration was investigated with the aid of anti-ED-1 antibody. On day 1 only a few ED-1–positive cells existed in the contusional lesions of both groups. On day 3, ED-1–positive cells had infiltrated extensively in the control group, but in the PP1 group they were restricted to the contusional lesion and its immediate surround (Fig. 4). The areas infiltrated by ED-1–positive cells in the control and PP1 groups were 10.52 ± 5.50 mm^2 ($n = 10$) and 4.07 ± 0.80 mm^2 ($n = 10$), respectively ($p < 0.005$); that is, the area of macrophage infiltration was significantly (approximately 60%) smaller in the PP1 group than in the control group. On day 7, the amount of macrophage infiltration was similar to that seen on day 3, but the area infiltrated by ED-1 positive cells in the control group was 7.95 ± 0.60 mm^2 ($n = 6$), which was smaller than on day 3. The area in the PP1 group on day 7 was 4.08 ± 0.15 mm^2 ($n = 6$), showing a significant difference between the two groups ($p < 0.005$; Fig. 5).

TNFα and IL-1β mRNA Expressions in the Injured Spinal Cord

In the control group, the fold-induction rate of expression of the gene encoding TNFα at 6 h after compression was 89.96 ± 53.23 ($n = 6$) compared with that seen in normal rats. In the PP1 group, however, the fold induction was significantly reduced to 42.00 ± 18.09 ($p < 0.005$, $n = 6$; Fig. 6a). The fold-induction rate of

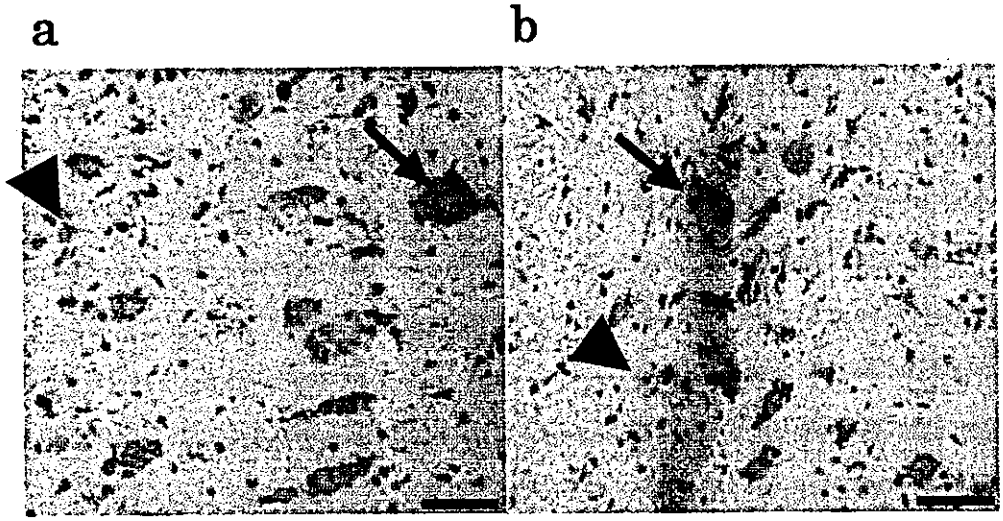

FIG. 1. Photomicrographs of VEGF immunohistochemical examination on day 3 after compression in the control group (**a**) and the PP1 group (**b**). VEGF protein expression was detected in the neurons (arrows) and glial cells (arrowheads) around the contusion in both groups. There was no statistical difference between the control and PP1 groups. Bar = 50 μm.

IL-1β mRNA expression at 6 h after compression was 288.19 ± 150.16 ($n = 8$) for the control group and 191.81 ± 79.90 ($n = 8$) for the PP1 group, a statistically significant difference ($p < 0.05$; Fig. 6b). These findings demonstrate that the expression of these genes was suppressed effectively by the administration of PP1.

DISCUSSION

Neurological deficits as a result of spinal cord trauma are due to both primary and secondary damage. Primary damage is primarily the result of direct mechanical injury to the spinal cord parenchyma as a, whereas secondary

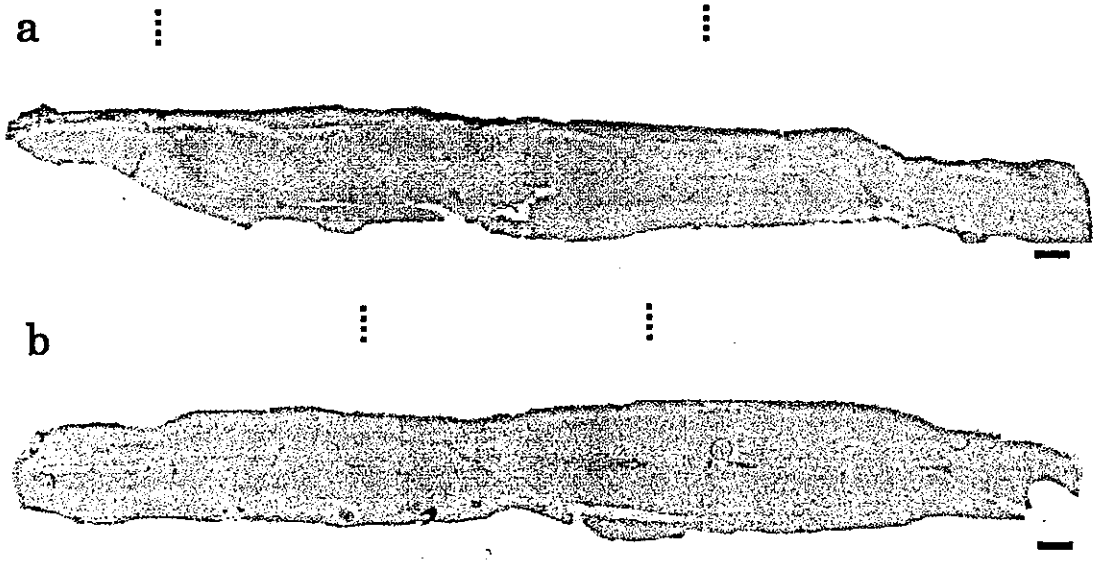

FIG. 2. Photomicrographs of anti-rat IgG immunohistochemical examination on day 1 after compression in the control group (**a**) and the PP1 group (**b**). Extent of edema (area between dotted lines), positive for IgG, was much less in the PP1 group than in the control group. Bar = 1 mm.

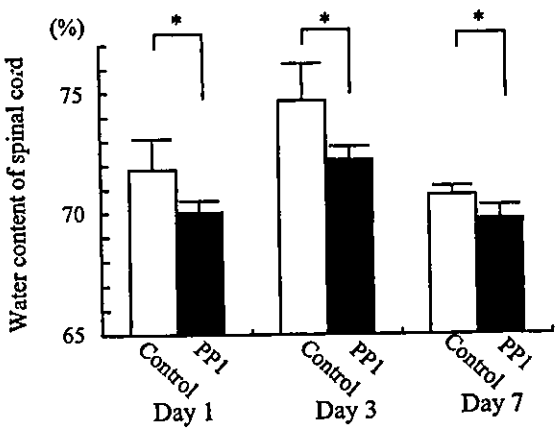

FIG. 3. Water content of the spinal cord in the control group and the PP1 group on days 1, 3, and 7 after compression. Values represent mean ± SD. Administration of PP1 significantly reduced the water content measured on all days ($*p < 0.05$).

damage may be initiated, for example, by an increase in vascular permeability, an increased inflammatory response, ischemia, excitatory amino acids, and free radicals (Ghirnikar et al., 2001; Topsakal et al., 2002). This study demonstrated that PP1 given 10 min after injury could reduce edema, the contusional area, macrophage infiltration, and inflammatory mediators after spinal cord compression injury in rats. The findings obtained with HE staining demonstrated that, although in both groups the severity of primary damage was virtually the same, in the control group the contusional area increased with time however, in contrast, PP1 attenuated this increase. Thus, PP1 can reduce secondary damage after spinal cord injury.

Similar levels of VEGF expression were observed in both the control and PP1 groups. Accordingly, Our results suggest that PP1 administration did not affect VEGF expression, which is consistent with the findings of a permanent MCA occlusion model (Kovács et al., 1996; Lennmyr et al., 1998) and a cerebral cold injury model (Nag et al., 1997). Moreover, the edema formation in our study indicated that the water content of the injured spinal cord peaked on day 3 in both groups and was reduced significantly by PP1 administration. Paul et al. (2001) reported that Src-deficient mice showed negligible vascular permeability in response to VEGF and were protected from edema-associated damage following stroke. Thus, Src may play a key role in VEGF-mediated edema formation.

In our opinion, VEGF may also contribute to edema formation in spinal cord injury, and the following mechanisms may be involved in this process. VEGF-induced stimulation of VEGF receptors (VEGFR) leads to the recruitment of Src and stimulation of its catalytic activity. Src is then activated by binding of the Src homology 2 domain to a tyrosine autophosphorylation site on VEGFR, and the activated Src may feed into a similar signaling pathway composed of phosphatidylinositol 3-kinase (PI-3K), phosphoinositide-dependent protein kinase (PDK), and Akt, leading to stimulation of endothelial cell survival, angiogenesis, and edema formation (Schlessinger, 2000). PP1, a widely applied, potent, and selective inhibitor of Src family tyrosine kinases, exerts its function by decreasing the phosphorylation of Src at Tyr^{416}, a known site of autophosphorylation (Hunter, 1987). Therefore, the mechanism of edema reduction observed in our study may be due to the suppression of Src family kinase function by PP1 after spinal cord injury.

Akt signaling mediates VEGF-induced vascular permeability (Six et al., 2002). The serine protein kinase Akt, that is located downstream of Src, is activated by PI-3K

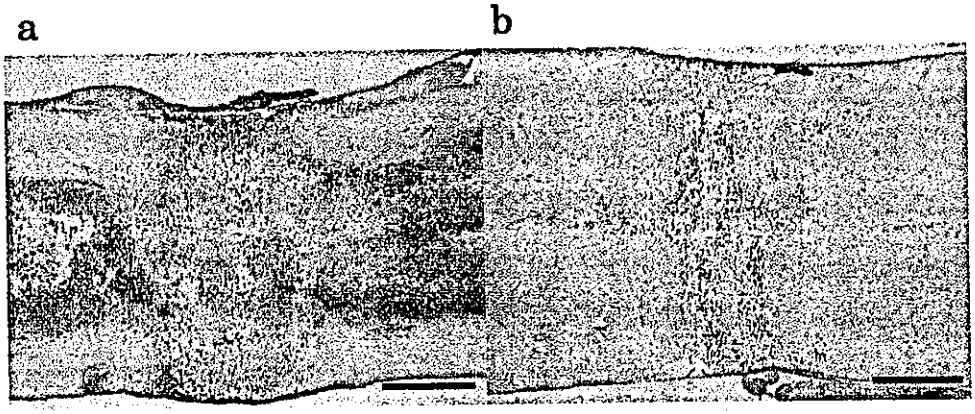

FIG. 4. Photomicrographs of ED-1 immunohistochemical examination on day 3 after compression in the control group (**a**) and the PP1 group (**b**). Abundant ED-1 positive cells were seen in the control group, but in the PP1 group they were restricted to the contusional area and its immediate surroundings. Bar = 1 mm.

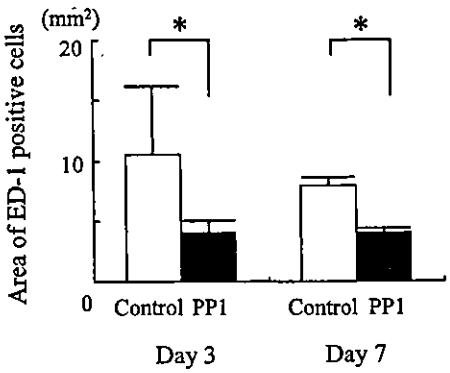

FIG. 5. Areas of ED-1 positive cell infiltration in the control group and the PP1 group on days 3 and 7 after compression. Values represent mean ± SD. The area of the ED-1 positive cell infiltration in the PP1 group was significantly smaller compared with that in the control group ($*p < 0.005$).

and promotes cell survival, angiogenesis, and vascular remodeling by mediating nitric oxide (NO) production (Fujio and Walsh, 1999; Fulton et al., 1999). Furthermore, PP1 may be involved in the PI-3K/Akt/NO pathway (Radisavljevic et al., 2000).

The area infiltrated by macrophages in our study peaked on day 3 in the control group. The administration of PP1 suppressed the infiltration of macrophages and restricted them to the area of the contusion and its immediate surround on days 3 and 7. Because PP1 reduced the extent of macrophage infiltration more dramatically than that of edema, it appears that reduction of inflammatory cells may be particularly important for neuroprotection.

PP1 inhibits the production of TNFα, IL-1β, and inducible NO synthase (iNOS) in murine macrophages stimulated with lipopolysaccharide (LPS) and interferon γ (IFNγ) (Orlicek et al., 1999; Lin et al., 2000). Macrophages and monocytes contain three major Src family kinases: Hck, Lyn, and Fgr (Meng and Lowell, 1997). Moreover, PP1 has been shown to inhibit Lyn with an IC_{50} approximately 30-fold lower than that of Src (Shah et al., 2002). It is therefore possible that, because PP1 blocks the activity of macrophages more strongly through the inhibition of Lyn, the overall inflammation response and the chemotaxis of macrophages are suppressed more strongly than edema formation.

Our study also demonstrated that PP1 suppressed the expression of TNFα and IL-1β mRNA in the injured spinal cord. These findings support the concept that the administration of PP1 effectively blocks gene expression related to early inflammatory response in spinal cord injury (Bartholdi and Schwab, 1997; Dinkel et al., 2003). In addition, PP1 may block the activity of Src family kinases to suppress macrophage activities that produce these cytokines, although we could not identify the cellular origins of TNFα and IL-1β.

Our results provide histological evidence that PP1 reduces secondary damage. The optimal timing and dosing of PP1 remain to be determined by evaluating both the histological and neurological effects of its administration. It's adverse effects must also be thoroughly investigated before considering the use of PP1 for the treatment of human spinal cord injury.

ACKNOWLEDGMENTS

We thank Dr. Shayne Morris, Department of Neurosurgery, Yukioka Hospital, for his very helpful advice and comments.

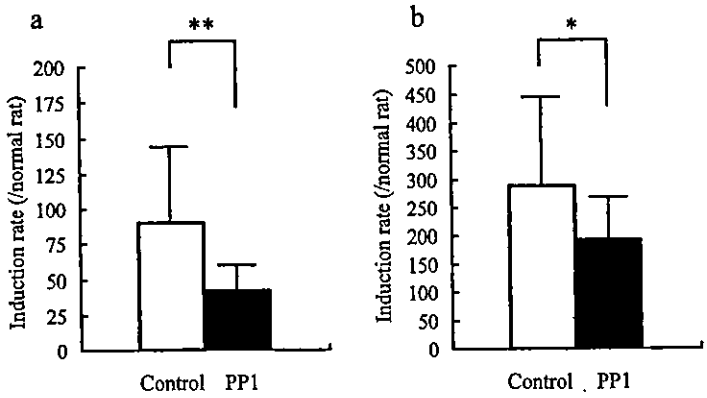

FIG. 6. Induction rate of mRNA in the rat spinal cord 6 h after compression: (a) TNFα mRNA and (b) IL-1β mRNA. The level of the mRNAs in these samples was normalized to the mRNA level of GAPDH, and the induction rates were calculated by comparing them with the levels in normal rat spinal cord. Values represent mean ± SD. PP1 significantly suppressed both TNFα and IL-1β mRNA ($*p < 0.05$, $**p < 0.005$).

REFERENCES

BARTHOLDI, D., and SCHWAB, M.E. (1997). Expression of pro-inflammatory cytokine and chemokine mRNA upon experimental spinal cord injury in mouse: an *in situ* hybridization study. Eur. J. Neurosci. **9,** 1422–1438.

BARTHOLDI, D., RUBIN, B.P., and SCHWAB, M.E. (1997). VEGF mRNA induction correlates with changes in the vascular architecture upon spinal cord damage in the rat. Eur. J. Neurosci. **9,** 2549–2560.

COBBS, C.S., CHEN, J., GREENBERG, D.A., et al. (1998). Vascular endothelial growth factor expression in transient focal cerebral ischemia in the rat. Neurosci. Lett. **249,** 79–82.

DEPRE, C., SHIPLEY, G.L., CHEN, W., et al. (1998). Unloaded heart in vivo replicates fetal gene expression of cardiac hypertrophy. Nat. Med. **4,** 1269–1275.

DINKEL, K., MACPHERSON, A., and SAPOLSKY, R.M. (2003). Novel glucocorticoid effects on acute inflammation in the CNS. J. Neurochem. **84,** 705–716.

EARNHARDT, J.N., STREIT, W.J., ANDERSON, D.K., et al. (2002). Induction of manganese superoxide dismutase in acute spinal cord injury. J. Neurotrauma **19,** 1065–1079.

ELICEIRI, B.P., PAUL, R., SCHWARTZBERG, P.L., et al. (1999). Selective requirement of Src kinases during VEGF-induced angiogenesis and vascular permeability. Mol. Cell **4,** 915–924.

FUJINAKA, T., KOHMURA, E., YUGUCHI, T., et al. (2003). The morphological and neurochemical effects of diffuse brain injury on rat central noradrenergic system. Neurol. Res. **25,** 35–41.

FUJIO, Y., and WALSH, K. (1999). Akt mediates cytoprotection of endothelial cells by vascular endothelial growth factor in an anchorage-dependent manner. J. Biol. Chem. **274,** 16349–16354.

FULTON, D., GRATTON, J.-P., McCABE, T.J., et al. (1999). Regulation of endothelium- derived nitric oxide production by the protein kinase Akt. Nature **399,** 597–601.

GHIRNIKAR, R.S., LEE, Y.L., and ENG, L.F. (2001). Chemokine antagonist infusion promotes axonal sparing after spinal cord contusion injury in rat. J. Neurosci. Res. **64,** 582–589.

HANKE, J.H., GARDNER, J.P., DOW, R.L., et al. (1996). Discovery of a novel, potent, and Src family-selective tyrosine kinase inhibitor. J. Biol. Chem. **271,** 695–701.

HE, H., HIROKAWA, Y., LEVITZKI, A., et al. (2000). An Anti-Ras cancer potential of PP1, an inhibitor specific for Src family kinases: *in vitro* and *in vivo* studies. Cancer J. **6,** 243–248.

HUNTER, T. (1987). A tail of two src's: mutatis mutandis. Cell **49,** 1–4.

KOVÁCS, Z., IKEZAKI, K., SAMOTO, K., et al. (1996). VEGF and flt expression time kinetics in rat brain infarct. Stroke **27,** 1865–1873.

LENNMYR, F., ATA, K.A., FUNA, K., et al. (1998). Expression of vascular endothelial growth factor (VEGF) and its receptors (Flt-1 and Flk-1) following permanent and transient occlusion of the middle cerebral artery in the rat. J. Neuropathol. Exp. Neurol. **57,** 874–882.

LIN, T., HIRJI, N., STENTON, G.R., et al. (2000). Activation of Macrophage CD8: pharmacological studies of TNF and IL-1β production. J. Immunol. **164,** 1783–1792.

MEDHURST, A.D., HARRISON D.C., READ S.J., et al. (2000). The use of TaqMan RT-PCR assays for semiquantitative analysis of gene expression in CNS tissue and disease models. J. Neurosci. Met. **98,** 9–20.

MENG, F., and LOWELL, C.A. (1997). Lipopolysaccharide (LPS)-induced macrophage activation and signal transduction in the absence of Src-family kinases Hck, Fgr, and Lyn. J. Exp. Med. **185,** 1661–1670.

NAG, S., TAKAHASHI, J.L., KILTY, D.W., et al. (1997). Role of vascular endothelial growth factor in blood–brain barrier breakdown and angiogenesis in brain trauma. J. Neuropathol. Exp. Neurol. **56,** 912–921.

ORLICEK, S.L., HANKE, J.H., and ENGLISH, B.K. (1999). The Src family-selective tyrosine kinase inhibitor PP1 blocks LSP and IFN-gamma-mediated TNF and iNOS production in murine macrophages. Shock **12,** 350–354.

PACZYNSKI, R.P., VENKATESAN, R., DIRINGER, M.N., et al. (2000). Effects of fluid management on edema volume and midline shift in a rat model of ischemic stroke. Stroke **31,** 1702–1708.

PAPAVASSILIOU, E., GOGATE, N., PROESCHOLDT, M., et al. (1997). Vascular endothelial growth factor (vascular permeability factor) expression in injured rat brain. J. Neurosci. Res. **49,** 451–460.

PAUL, R., ZHANG, Z.G., ELICEIRI, B.P., et al. (2001). Src deficiency or blockade of Src activity in mice provides cerebral protection following stroke. Nat. Med. **7,** 222–227.

PLATE, K.H., and RISAU, W. (1995). Angiogenesis in malignant gliomas. Glia **15,** 339–347.

RADISAVLJEVIC, Z., AVRAHAM, H., and AVRAHAM, S. (2000). Vascular endothelial growth factor up-regulates ICAM-1 expression via the phosphatidylinositol 3 OH-kinase/AKT/nitric oxide pathway and modulates migration of brain microvascular endothelial cells. J. Biol. Chem. **275,** 20770–20774.

SCHLESSINGER, J. (2000). New role for Src kinases in control of cell survival and angiogenesis. Cell **100,** 293–296.

SENGER, D.R., GALLI, S.J., DVORAK, A.M., et al. (1983). Tumor cells secrete a vascular permeability factor that promotes accumulation of ascites fluid. Science **219,** 983–985.

SHAH, O.J., KIMBALL, S.R., and JEFFERSON, L.S. (2002).

The Src-family tyrosine kinase inhibitor PP1 interferes with the activation of ribosomal protein S6 kinases. Biochem. J. **366,** 57–62.

SIX, I., KUREISHI, Y., LUO, Z., et al. (2002). Akt signaling mediates VEGF/VPF vascular permeability *in vivo*. FEBS. Lett. **532,** 67–69.

SKÖLD, M., CULLHEIM, S., HAMMARBERG, H., et al. (2000). Induction of VEGF and VEGF receptors in the spinal cord after mechanical spinal injury and prostaglandin administration. Eur. J. Neurosci. **12,** 3675–3686.

SUZUKI, Y., MATSUMOTO, Y., IKEDA, Y., et al. (2002). SM-20220, a Na^+/H^+ exchanger inhibitor: effects on ischemic brain damage through edema and neutrophil accumulation in rat middle cerebral artery occlusion model. Brain. Res. **945,** 242–248.

TOPSAKAL, C., EROL, F.S., OZVEREN, M.F., et al. (2002). Effects of methylprednisolone and dextromethorphan on lipid peroxidation in an experimental model of spinal cord injury. Neurosurg. Rev. **25,** 258–266.

UENO, T., SAWA, Y., KITAGAWA-SAKAKIDA, S., et al. (2001). Nuclear factor-κB decoy attenuates neuronal damage after global brain ischemia: a future strategy for brain protection during circulatory arrest. J. Thorac. Cardiovasc. Surg. **122,** 720–727.

Address reprint requests to:
Takamichi Yuguchi, M.D., Ph.D.
Department of Neurosurgery
Spine and Spinal Cord Center
Yukioka Hospital
2-2-3 Ukita Kita-ku
Osaka City, Osaka 530-0021, Japan

E-mail: yuguchi@yukioka.or.jp

The morphological and neurochemical effects of diffuse brain injury on rat central noradrenergic system

Toshiyuki Fujinaka, Eiji Kohmura, Takamichi Yuguchi and Toshiki Yoshimine

Department of Neurosurgery, Osaka University Medical School, Osaka, Japan

The central noradrenergic system is widely distributed throughout the brain and is closely related to spontaneous motility and level of consciousness. The study presented here evaluated the morphological as well as neurochemical effects of diffuse brain injury on the central noradrenergic system in rat. Adult male Sprague–Dawley rats were subjected to impact–acceleration brain injury produced with a weight-drop device. Morphological changes in locus coeruleus (LC) neurons were examined by using immunohistochemistry for dopamine-β-hydroxylase, and norepinephrine (NE) turnover in the cerebral cortex was measured by high performance liquid chromatography with electrochemical detection. The size of LC neurons increased by 11% 24 h after injury but had decreased by 27% seven days after injury. Axons of noradrenergic neurons were swollen 24 h and 48 h after injury but the swelling had dwindled in seven days. NE turnover was significantly reduced seven days after injury and remained at a low level until eight weeks after injury. These results suggest that focal impairment of axonal transport due to diffuse brain injury causes cellular changes in LC and that the neurochemical effect of injury on the central noradrenargic system lasts over an extended period of time. Chronic suppression of NE turnover may explain the sustained behavioral and psychological abnormalites observed in a clinical situation. [Neurol Res 2003; 25: 35–41]

Key Words: Locus coeruleus; diffuse brain injury; norepinephrine (NE); 3-methoxy-4-hydroxyphenylglycol (MHPG); dopamine-β-hydroxylase

INTRODUCTION

Protracted disturbance of consciousness and lowered motility are the major problems in patients who survive severe head injury. Neuropsychological deficits prevent them from returning to a normal life even if they have physically recovered. Various neurotransmitter pathways in the central nervous systems are likely to be damaged in diffuse brain injury, and alterations in neurotransmitters may be the main cause of psychological and behavioral abnormalities after diffuse brain injury.

The central noradrenergic system, distributed widely throughout the brain, is closely related to changes in activity and level of consciousness in post-traumatic subjects[1–8]. Recent studies suggest that the release and turnover of norepinephrine (NE) are affected by traumatic brain injury, the mode and severity being dependent on various factors such as the type, site and side of injury, time after injury and site of assesment[9–14]. Recent studies have also indicated that central NE facilitates functional recovery after various types of experimental brain injury such as sensorimotor cortex ablation, cerebral contusion or fluid percussion injury[15–21]. In a rat model of local brain injury, NE release and turnover increased during the first few hours and then started to decrease 24 h after injury[13,22,23]. These effects of injury on the central noradrenergic system may play a major role in the disturbance of consciousness and behavioral deficits following diffuse brain injury. In the present study, the effects of diffuse brain injury on the central noradrenergic system were investigated in rats. The morphological changes in the central noradrenergic system were evaluated in the locus coeruleus (LC) neurons and the neurochemical changes were assessed in terms of NE metabolism.

MATERIALS AND METHODS

Diffuse brain injury model

An impact–acceleration injury model was produced according to the method of Marmarou *et al.*[24,25] with modifications. Adult male Sprague–Dawley rats weighing 500–550 g were anesthetized with intraperitoneal chloral hydrate (350 mg kg^{-1}), and an additional injection was administered during the experiment if needed. A midline scalp incision was made and periosteum was reflected to expose the skull between the coronal and lambdoid sutures. A metallic disc 20 mm in diameter and 1.5 mm thick was secured to the exposed skull

Correspondence and reprint requests to: Toshiyuki Fujinaka, MD, Department of Neurosurgery, Osaka University Medical School, 2-2 Yamadaoka, Suita, Osaka 565-0871, Japan. [fujinaka@nsurg.med.osaka-u.ac.jp] Accepted for publication July 2002.

0161-6412/03/010035-07

vertex with cyanoacrylic glue. The animals were then placed in the prone position on a form bed while breathing spontaneously. Impact–acceleration brain injury was achieved with a weight-drop device. A brass weight (450 g) was dropped freely by force of gravity from a height of 1.5 m onto the metallic disc. The rat was moved away immediately following the initial impact to avoid a second insult and then observed for several minutes. After removal of the disc, the scalp was sutured and the rat was returned to its cage (injury group). For the control group, rats were treated as described above except for receiving impact.

All animal experiments were conducted in compliance with the Osaka University Medical School Guidelines for the Care and Use of Laboratory Animals. Animal surgery and the experimental procedure were approved by the Committee for Animal Care and Use, Osaka University Medical School.

Brain fixation and immunohistochemistry

The animals were anesthetized 1, 2, 7, 14, 28, and 56 days after injury and perfused intracardially first with saline and then with 4% paraformaldehyde in 0.1 M phosphate buffer. Four animals each from the injury and control groups were used for each experimental period. The brains were removed and post-fixed with the same fixative for 24 h at 4°C. After immersion in 30% sucrose in 0.01 M phosphate buffered saline (PBS), the brains were embedded in Tissue-Tech and stored at −80°C. Fixed brains were sliced into 12 μm serial coronal sections from 8 mm to 11 mm posterior to the bregma, including the LC, with a freezing microtome and processed for immunohistochemistry.

Immunohistochemistry was used to identify dopamine-β-hydroxylase (DBH) and neurofilaments. Sections were washed in PBS and permeabilized with acetone at −20°C for 10 min, incubated with 0.3% hydrogen peroxide for 30 min to quench intrinsic peroxidase, and washed three times for 5 min each in PBS. Blocking of nonspecific binding was achieved with 2% normal horse serum in a buffer (0.1% Triton X-100 and 5% sucrose in PBS) for 20 min, and sections were finally incubated overnight at 4°C with the primary antibodies. The antibodies used for the immunohistochemical studies were anti dopamine-β-hydroxylase rabbit polyclonal antibody (Eugene Tech International, Ridgefield Park, NJ, USA; diluted 1 : 1000) and anti-68kD-neurofilament mouse monoclonal antibody (Boehringer Mannheim Biochemica, Germany; diluted 1 : 50). The sections were washed in PBS three times for 5 min each, incubated with biotinylated anti-mouse-rabbit IgG (Vectastain Elite ABC Universal Kit, Vector Laboratories, Inc., Burlingame, CA, USA; diluted 1 : 200) for 60 min, and after three 5-min washes in PBS, re-incubated with avidin–biotin peroxydase complex (Vectastain Elite ABC Kit; diluted 1 : 100) for 60 min. Immunolabeled structures were visualized with 0.05% 3,3′-diamino-benzidine tetrahydrochloride (DAB) and 0.01% hydrogen peroxide in PBS. The precipitate formed by DAB was enhanced with 0.8% $NiCl_2$ in PBS. Finally, the sections were washed in water and dehydrated in ethanol for mounting.

Measurement of cellular size

Every fifth serial coronal section immunostained with DBH was assessed to evaluate the changes in cellular size in the LC. The microscopic images of the LC were captured with a digital camera (Fujix HC-300; Fujifilm) mounted on a microscope with 20 objective lens, and stored in a computer. The cross sectional area of each of the stained neurons was measured with the aid of an image-analysis program (Scion Image, Scion Corp., Frederick, MD, USA). Only the stained area containing the nucleus was measured to avoid the cut edge, and measurements were averaged for all sections from one side of the LC and shown as a percentage of control animals. The data were expressed as mean ± SEM values. Statistical differences in the cellular size between the experimental and control groups were assessed by an analysis of variance (ANOVA) with the Newman-Keuls test for intergroup multiple comparisons. Differences were considered to be statistically significant at p-values of 0.05 or less.

Quantitative measurement of brain catecholamines

The tissue levels of NE and 3-methoxy-4-hydroxyphenylglycol (MHPG), the major extracellular metabolite of NE, in the bilateral cerebral cortex were measured by using high performance liquid chromatography with electrochemical detection (HPLC–ED). Animals from the experimental and control groups were decapitated under deep anesthesia 2, 7, 14 and 56 days after injury ($n = 6$–10 for each time point). The brains were quickly removed and the cortices dissected. Tissue samples were immediately frozen in liquid nitrogen and stored at −80°C until quantitative measurement of the brain catecholamines. These samples were weighed and initially added to 1 ml per 100 mg of 0.1 M perchloric acid containing 0.1 mM of sodium pyrosulfite and 0.02 mM of ethylenodiamine tetra-acetic acid disodium salt (EDTA 2Na). The mixture was then homogenized with an ultrasonic cell disruptor at 0°C for 30 sec and centrifuged at 12,000 rpm for 20 min at 0°C. The supernatant was filtered through a 0.45 μm centrifugal filter at 12,000 rpm for 15 mins at 0°C to separate the insoluble residue. A portion of the supernatant was then further centrifuged at 20,000 rpm for 2 min and an aliquot of the supernatant was injected into the HPLC–ED system. The HPLC–ED system was similar to that described by Takeda *et al.*[26]. The mobile phase was prepared with 50 mM disodium hydrogenphosphate 12-water, 50 mM citric acid, 4.4 mM sodium l-heptanesulphonate, 0.1 mM EDTA 2Na, 7.7% methanol and 3.1% asetonitrile, pH 3.0. This was run over a MCM C_{18} 5 μm column (150 mm×4.6 mm i.d.) with a flow rate of 0.9 ml min^{-1} at 23°C. The conditioning cell was set at 350 mV and the analytical cell (dual coulometric working electrodes) at 80 mV and 350 mV.

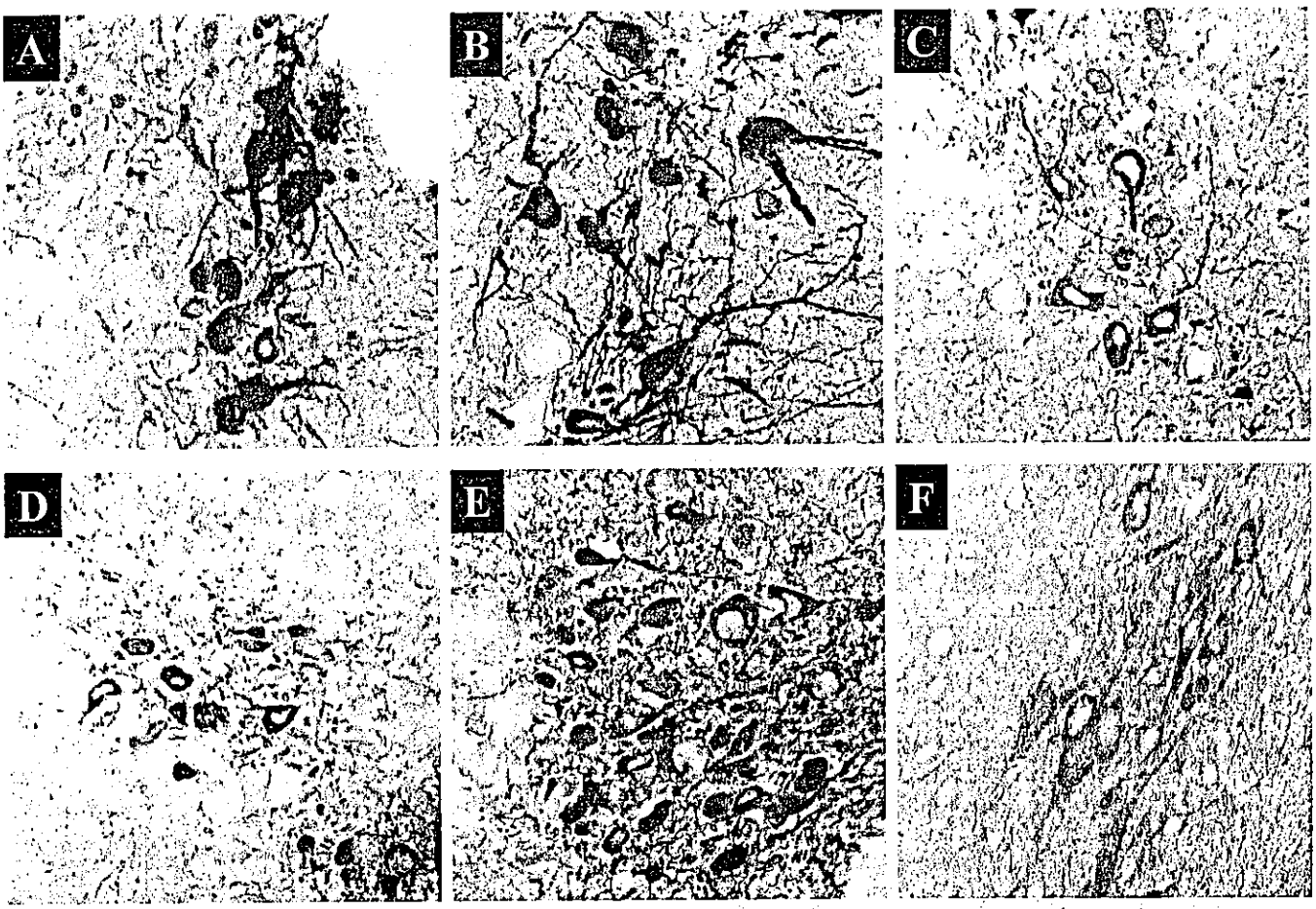

Figure 1: Photomicrographs of locus coeruleus (LC) immunostained with anti-dopamine-β-hydroxylase (DBH) in **A:** control animal, **B:** 24 h after injury, **C:** one week after injury, **D:** two weeks after injury, **E:** four weeks after injury, **F:** eight weeks after injury. Shrinkage of LC neurons immunostained with DBH was observed one and two weeks after injury. Four and eight weeks after injury, LC neurons were the same size as those of control animals

NE turnover was defined as the ratio of MHPG to NE levels[27,28]. For each of the experimental animals, this ratio was displayed as a percentage of the average for control animals, and expressed as mean ± SEM values. Statistical differences in the NE turnover between the experimental and control groups were assessed by ANOVA with the Newman–Keuls test for intergroup multiple comparisons. For this analysis, NE turnover values from both sides of the cortices were averaged together, and differences between the sides at each time point were analyzed with a *t*-test. A *p*-value of 0.05 or less was regarded as statistically significant.

RESULTS

Seventy-seven rats underwent the impact–acceleration brain injury. The mortality immediately after the injury was 19.5% (15/77). Post-traumatic seizure was observed in 39 (62.8%) of the surviving animals. Recovery from anesthesia took longer for injured animals than for control animals. Spontaneous motility in the survivors was reduced after recovery from anesthesia. Body weight was reduced to 86.6 ± 2.52% one week after injury and recovered to 100.7 ± 9.16% in four weeks. Subarachnoid and intraventricular hemorrhages were frequently observed, but skull fracture and contusion did not occur in any animals throughout the experiment. Immunohistochemistry for anti-68kD-neurofilament showed extensive axonal injury particularly in the ventral and central brain stem one or two days after injury.

Immunohistochemistry for DBH showed that the size of the LC neurons tended to increase initially one day after injury but thereafter decreased in size. One week after injury, LC neurons immunostained with DBH were noticeably smaller than those of control animals. No significant loss of cells was observed in the LC, and four and eight weeks after injury, the LC neurons were the same size as those of control animals (*Figure 1*). The axons of the LC neurons and the dorsal catecholamine bundles, the projection pathway of noradrenergic

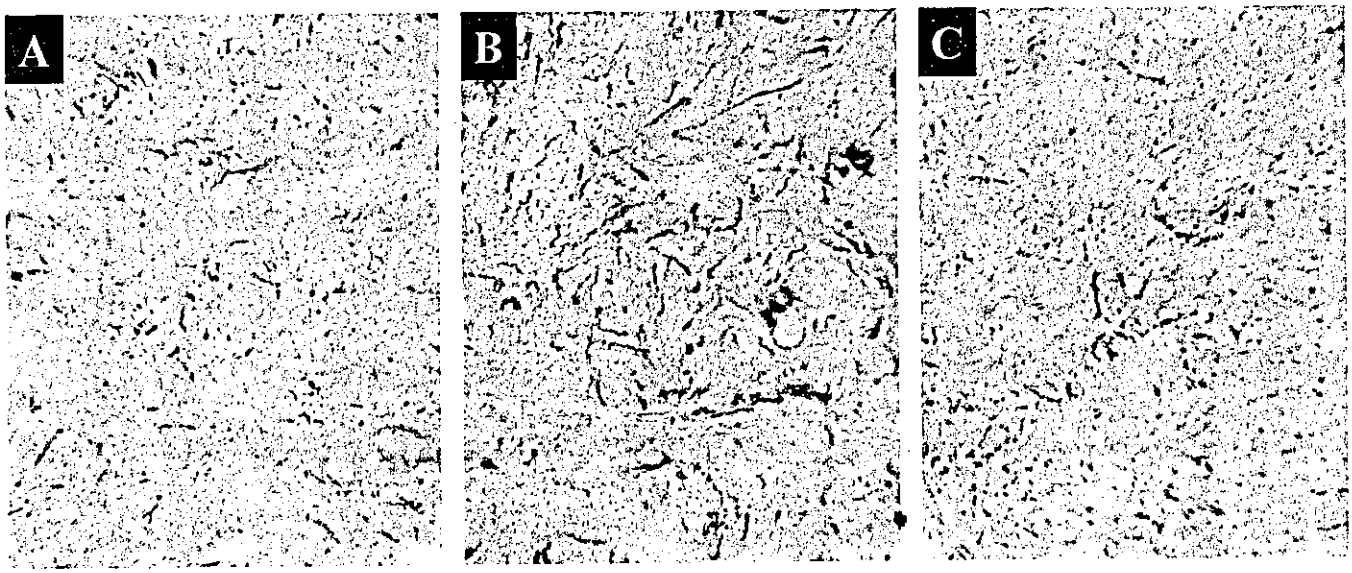

Figure 2: Photomicrographs of dorsal catecholamine bundles immunostained with anti-dopamine-β-hydroxylase in **A:** control animal, **B:** 24 h after injury, **C:** one week after injury. The axons of the dorsal catecholamine bundles were swollen 24 h after injury but the swelling had dwindled in one week

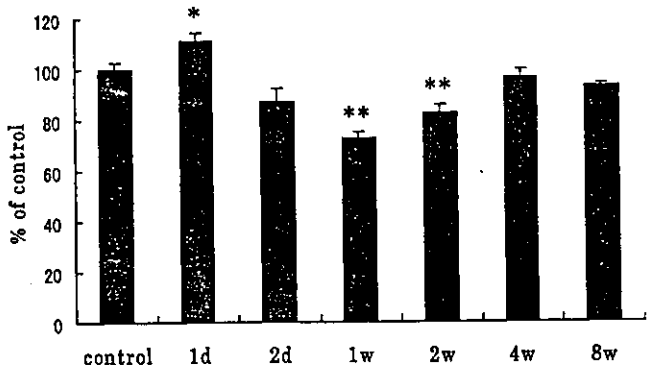

Figure 3: Cross-sectional area of locus coeruleus (LC) neurons immunostained with anti-dopamine-β-hydroxylase. Data are shown as a percentage of control animals. The values are means ± SEM, $*p<0.05$, $**p<0.01$

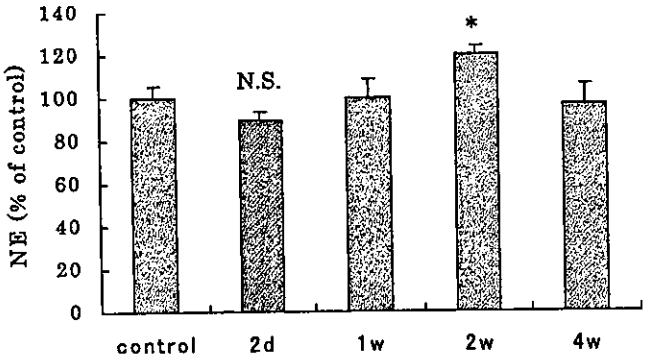

Figure 4: Total amount of norepinephrine (NE) in the cortex. Data are shown as a percentage of control animals. The values are means ± SEM. * indicates $p<0.05$

neurons, were swollen 24 h and 48 h after injury but the swelling had dwindled in seven days (*Figure 2*). Quantitative image analysis confirmed these findings. The size of the LC neurons immunostained with DBH increased by 11.2 ± 3.58% ($p<0.05$ compared to control) 24 h after injury. The mean size of the LC neurons immunostained with DBH decreased to 72.9 ± 2.07% ($p<0.01$ compared to control) seven days after injury and to 82.4 ± 3.71% ($p<0.01$ compared to control) 14 days after injury. Four and eight weeks after injury, the size had returned to near control value (*Figure 3*).

Tissue levels of NE and MHPG were measured with HPLC–ED. Total amount of NE in the cortex was not reduced during the experimental period, and two weeks after injury it had significantly increased ($p<0.05$ compared to control) (*Figure 4*). Norepinephrine turnover, defined as the ratio of MHPG to NE levels and shown as a percentage of that of control animals, had not changed in the cortex two days after injury, but decreased significantly one, two and eight weeks after injury ($p<0.01$ compared to control). One week after injury, NE turnover was 22.6 ± 3.38% of control value, and then gradually increased but remained significantly low even eight weeks after injury. No significant difference in NE turnover was found between the cerebral cortices on either side throughout the experiment (*Figure 5*).

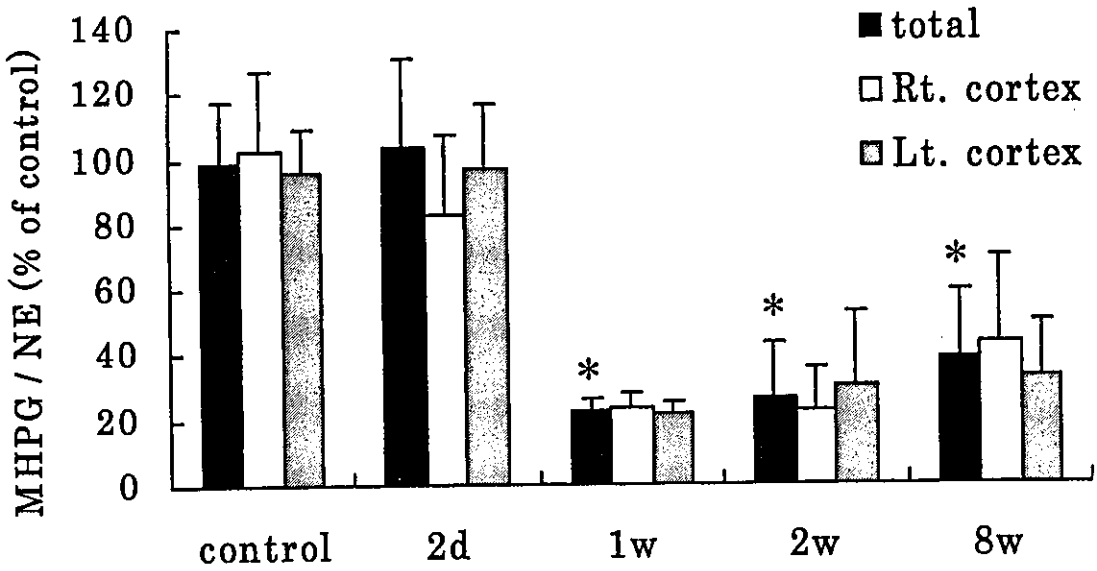

Figure 5: Norepinephrine (NE) turnover displayed as a percentage of control animals. NE turnover is defined as the ratio of 3-methoxy-4-hydroxyphenylglycol (MHPG) to NE levels. Data are shown as a percentage of control animals. The values are means ± SEM. * indicates $p < 0.01$

DISCUSSION

Marmarou *et al.*[24,25] described an experimental model capable of producing diffuse brain injury in the rodent. As the original method when used by us resulted in high mortality and high frequency of skull fracture, we modified a few points for our study. We used a metallic disc 20 mm in diameter and the weight was dropped from a height of 1.5 m. Immediate mortality was about 20%. Histological examination revealed typical signs of diffuse axonal damage particularly in the brainstem without apparent contusional damage underneath the disc.

We examined the central noradrenergic system following impact–acceleration brain injury. The locus coeruleus is a nucleus located in the tegmentum of the upper pons and consists mainly of pigmented neurons which contain norepinephrine. The noradrenergic pathways originating from the LC influence neural activities in many cortical regions of the brain and also distribute to subcortical structures, including the hypothalamus, hippocampus and cerebellar cortex[1–8]. Previous studies have suggested important roles for norepinephrine in the functional recovery after focal traumatic brain injury. Central norepinephrine concentration or its turnover decreased in the early phase after brain injury produced by either weight drop or cortical impact[13,19,22]. Intraventricular administration of norepinephrine could improve motor function after unilateral sensorimotor cortex ablation[15]. Drugs with an antagonistic effect on alpha 1 NE receptors, including haloperidol and prazosin, when administered early after a traumatic unilateral focal contusion in the sensorimotor cortex, retarded locomotor recovery[17,29]. Pre-treatment with the noradrenergic neurotoxin DSP-4 significantly retarded motor recovery in animals after unilateral sensorimotor cortex ablation[30]. Administration of L-threo-3,4-dihydroxyphenylserine, a precursor of NE, with benserazide, a peripheral aromatic amino acid decarboxylase inhibitor, promoted the recovery of locomotor function after unilateral sensorimotor cortex ablation injury[31].

Our study demonstrated the shrinkage of LC neurons in a diffuse brain injury model. The size of the LC neurons initially tended to increase by about 11% 24 h after injury, and the axons of noradrenergic neurons were swollen 24 h and 48 h after injury. These findings suggest that focal impairment of anterograde axonal transport due to diffuse brain injury induced initial cellular swelling of the LC neurons, but they decreased in size by about 27% seven days after injury but they returned to control value four and eight weeks after injury. Our impact–acceleration brain injury caused the initial swelling and following shrinkage of the LC neurons, but they recovered spontaneously within four weeks. LC neurons are known to have a strong regenerative response[32–35]. Administration of noradrenergic neurotoxin DSP-4 induced the initial cell loss in the LC and enhanced the sprouting from surviving neurons[35]. It is possible that these regenerative reactions were also induced in our model.

On the other hand, Carbary *et al.*[36] reported that no discernible qualitative differences were found between control and experimental animals in the intensity of immunostaining for either tyrosine or dopamine-β-hydroxylase in the ipsilateral LC 24 h or seven days after moderate fluid percussion injury. The biosynthesis of NE in the LC might not be affected by experimental moderate focal brain injury. Arakawa *et al.*[37] reported that changed EEG and LC neuronal activities recovered to pre-injury levels within 1 h after diffuse brain injury.

Their impact–acceleration injury model was produced with a 400 g weight dropped from a height of 1 m and all animals survived the impact–acceleration injury. Differences in the type and severity of injury may well be responsible for differences in cellular reaction.

Besides morphologic alterations in the LC neurons, the changes in NE metabolism are also related to disturbance of cortical functions[38–40]. We measured the tissue concentrations of NE and MHPG and calculated the ratio of MHPG to NE to reflect NE turnover[27,28]. With focal brain contusion, NE turnover was either eliminated or reduced bilaterally by 45%–92% in the cerebral cortex, hypothalamus, cerebellum, LC and medulla 24 h after injury[13]. With unilateral cerebral contusion, NE turnover initially and briefly increased 30 min after injury followed by bilateral widespread depression 6–24 h after injury[41]. In our study, NE turnover had not changed significantly in the cortex 48 h after injury, but had decreased significantly one week after injury. Although it was not examined whether NE turnover was affected in the chronic phase of the injury in the previous reports, we found that it remained at a very low level even eight weeks after injury. We did not observe any initial changes in NE turnover but our data showed prolonged depression of NE turnover in the chronic phase. The different nature of the experimental model and severity of injury may explain the differences in NE turnover. Whether NE turnover continued to decrease in the focal injury model is not clear. Two possible mechanisms might be involved in the prolonged impairment in NE turnover, loss of NE fibers projecting from the LC neurons or depression of NE synaptic activity. Although our study demonstrated that the LC neurons were affected in the early phase as was shown by the reduction in size one to two weeks after injury, they recovered their size four to eight weeks after injury. Damaged NE fibers are thus likely to recover in the chronic phase. Indeed, the total content of NE in the cortex was not reduced but rather increased two weeks after injury. However, NE turnover which remained affected one to two weeks after injury did not recover in the chronic phase (eight weeks after injury) either, which indicates prolonged depression of cortical synaptic activity. Details of the mode of impairment of this important neurotransmission system are not clear at present. Further clarification of the pathophysiology of the central noradrenergic system is considered indispensable for the development of optimal management of patients with diffuse brain injury in order to facilitate neuropsychological recovery.

REFERENCES

1 Olsen L, Fuxe K. On the projections from the locus coeruleus noradrenaline neurons: The cerebellar innervation. *Brain Res* 1971; **28**: 165–171
2 Kobayashi RM, Palkovits M, Kopin IJ, Jacobowitz DM. Biochemical mapping of noradrenergic nerve arising from rat locus coeruleus. *Brain Res* 1974; **77**: 269–279
3 Crow TJ, Deakin JFW, File SE, Longden A, Wendlandt S. The locus coeruleus noradrenergic system – evidence against a role in attention, habituation anxiety and motor activity. *Brain Res* 1978; **155**: 249–261
4 Foote SL, Bloom FE, Aston-Jones G. Nucleus locus coeruleus: New evidence of anatomical and physiological specificity. *Physiol Rev* 1983; **63**: 844–914
5 Saper CB. Function of the locus coeruleus. *Trends Neurosci Lett* 1987; **10**: 343–344
6 Sakaguchi T, Nakamura S. The mode of projections of single locus coeruleus neurons to the cerebral cortex in rats. *Neuroscience* 1987; **20**: 221–230
7 Fritschy JM, Grzanna R. Distribution of locus coeruleus axons within the rat brainstem demonstrated by Phaseolus vulgaris leucoagglutinin anterograde tracing in combination with dopamine-beta-hydroxylase immunofluorescence. *J Comp Neurol* 1990; **291**: 616–631
8 Petrov T, Krukoff TL, Jhamandas JH. Branching projections of catecholaminergic brainstem neurons to the paraventricular hypothalamic nucleus and the central nucleus of the amygdala in the rat. *Brain Res* 1993; **609**: 81–92
9 Huger F, Patrick G. Effect of concussive head injury on central catecholamine levels and synthesis-rates in rat brain regions. *J Neurochem* 1979; **33**: 89–95
10 Levin BE. Alterations of norepinephrine metabolism in rat locus coeruleus neurons in response to axonal injury. *Brain Res* 1983; **289**: 205–214
11 Globus MYT, Busto R, Dietrich WD, Martinez E, Valdés I, Ginsberg MD. Direct evidence for acute and massive norepinephrine release in the hippocampus during transient ischemia. *J Cereb Blood Flow Metab* 1989; **9**: 892–896
12 Sutton RL, Krobert KA. Acute changes in cortical noradrenaline levels of the anesthetized rat following cortical contusion: A microdialysis study. *J Neurotrauma* 1993; **10**: S181
13 Dunn-Meynell A, Pan S, Levin BE. Focal traumatic brain injury causes widespread reductions in rat brain norepinephrine turnover from 6 to 24 h. *Brain Res* 1994; **660**: 88–95
14 Levin BE, Pan S, Dunn-Meynell A. Chronic alterations in rat brain α-adrenoceptors following traumatic brain injury. *Restor Neurol Neurosci* 1994; **7**: 5–12
15 Boyeson MG, Feeney DM. Intraventricular norepinephrine facilitates motor recovery following sensorimotor cortex injury. *Pharmacol Biochem Behav* 1990; **35**: 497–501
16 Goldstein LB, Davis JN. Post-lesion practice and amphetamine-facilitated recovery of beam-walking in the rat. *Restor Neurol Neurosci* 1990; **1**: 311–314
17 Feeney DM, Westerberg VS. Norepinephrine and brain damage: Alpha noradrenergic pharmacology alters functional recovery after cortical trauma. *Can J Psychol* 1990; **44**: 233–252
18 Goldstein LB, Coviello A, Miller GD, Davis JN. Norepinephrine depletion impairs motor recovery following sensorimotor cortex injury in the rat. *Restor Neurol Neurosci* 1991; **3**: 41–47
19 Krobert KA, Sutton RL, Feeney DM. Spontaneous and amphetamine-evoked release of cerebellar noradrenaline after sensorimotor cortex contusion: An *in vivo* microdialysis study in the awake rat. *J Neurochem* 1994; **62**: 2233–2240
20 Sutton RL, Feeney DM. α-Noradrenergic agonists and antagonists affect recovery and maintenance of beam-walking ability after sensorimotor cortex ablation in the rat. *Restor Neurol Neurosci* 1992; **4**: 1–11
21 Prasad MR, Dose JM, Dhillon HS, Carbary T, Kraemer PJ. Amphetamine affects the behavioral outcome of lateral fluid percussion brain injury in the rat. *Restor Neurol Neurosci* 1995; **9**: 65–75
22 Prasad MR, Ramaiah C, Mcintosh TK, Dempsey RJ, Hipkens S, Yurek D. Regional levels of lactate and norepinephrine after experimental brain injury. *J Neurochem* 1994; **63**: 1086–1094
23 Levin BE, Brown KL, Pawar G, Dunn-Meynell A. Widespread and lateralized effects of acute traumatic brain injury on norepinephrine turnover in the rat brain. *Brain Res* 1995; **674**: 307–313
24 Marmarou A, Foda MAAE, van den Brink W, Campbell J, Kita H, Demetriadou K. A new model of diffuse brain injury in rats. Part 1: Pathophysiology and biomechanics. *J Neurosurg* 1994; **80**: 291–300
25 Foda MAAE, Marmarou A. A new model of diffuse brain injury in

rats, Part II: Morphological characterization. *J Neurosurg* 1994; **80**: 301–313
26 Takeda H, Matsumiya T, Shibuya T. Detection and identification modes for the highly sensitive and simultaneous determination of various biogenic amines by coulometric high-performance liquid chromatography. *J Chromatogr* 1990; **515**: 265–278
27 Schanberg SM, Schildkraut JJ, Breese GR, Kopin IJ. Metabolism of normetanerphrine-H3 in rat brain identification of conjugated 3-methoxy-4-hydroxyphenylglycol as the major metabolite. *Biochem Pharmacol* 1968; **17**: 247–254
28 Westerink BHC. Determination of normetanephrine, 3,4-dihydroxyphenylethyleneglycol (free and total), and 3-methoxy-4-hydroxyphenylethyleneglycol (free and total) in rat brain by high-performance liquid chromatography with electrochemical detection and effects of drugs on regional concentrations. *J Neurochem* 1984; **42**: 934–942
29 Dunn-Meynell AA, Yarlagadda Y, Levin BE. α1-adrenoceptor blockade increases behavioral deficits in traumatic brain injury. *J Neurotrauma* 1997; **14**: 43–52
30 Boyeson MG, Callister TR, Cavazos JE. Biochemical and behavioral effects of a sensorimotor cortex injury in rats pretreated with the noradrenergic neurotoxin DSP-4. *Behav Neurosci* 1992; **106**: 964–973
31 Kikuchi K, Nishino K, Ohyu H. Increasing CNS norepinephrine levels by the precursor L-DOPS facilitates beam-walking recovery after sensorimotor cortex ablation in rats. *Brain Res* 2000; **860**: 130–135
32 Stenevi U, Björklund A, Moore RY. Growth of intact adrenergic axons in the denervated lateral geniculate body. *Exp Neurol* 1972; **35**: 290–299
33 Nakai K, Jonsson G, Kasamatsu T. Norepinephrinergic reinnervation of cat occipital cortex following localized lesion with 6-hydroxydopamine. *Neurosci Res* 1987; **4**: 433–453
34 Nakai K. Regenerative catecholamine-containing terminals in kitten visual cortex: An ultrastructual study. *Neurosci Res* 1987; **4**: 475–485
35 Fritschy JM, Grazanna R. Restoration of ascending noradrenergic projections by residual locus coeruleus neurons: Compensatory response to neurotoxin-induced cell death in the adult rat brain. *J Comp Neurol* 1992; **321**: 421–441
36 Carbary T, Dhillon HS, Scheff SW, Prasad RM. Immunohistochemistry of tyrosine and dopamine-β-hydroxylases after experimental brain injury in the rat. *Neurosci Res Comm* 1996; **18**: 79–85
37 Arakawa S, Nakamura S, Kawashima N, Nishiike S, Okuyama S. Antagonizing effects of VA-045 on reduced activity of rat locus coeruleus neurons following head injury or intravenous injection of clonidine. *Life Sci* 1995; **57**: 1803–1810
38 Foote SL, Aston-Jones G, Bloom FE. Impulse activity of locus coeruleus neurons in awake rats and monkeys is a function of sensory stimulation and arousal. *Proc Natl Acad Sci USA* 1980; **77**: 3033–3037
39 Aston-Jones G, Bloom FE. Norepinephrine-containing locus coeruleus neurons in behaving rats exhibited pronounced responses to non-noxious environmental stimuli. *J Neurosci* 1981; **1**: 887–900
40 Berridge CW, Page ME, Valentino RJ, *et al.* Effect of locus coeruleus inactivation on electroencephalographic activity in neocortex and hippocampus. *Neuroscience* 1993; **55**: 381–393
41 Dunn-Meynell AA, Hassanain M, Levin BE. Norepinephrine and traumatic brain injury: A possible role in post-traumatic edema. *Brain Res* 1998; **800**: 245–252